ON THE TORQUE AND WEAR BEHAVIOR OF SELECTED THIN FILM MOS_2 LUBRICATED GIMBAL BEARINGS*

John J. Bohner and Peter L. Conley**

ABSTRACT

During the thermal vacuum test phase of the GOES 7 spacecraft, the primary scan mirror system exhibited unacceptably high drive friction. The observed friction was found to correlate with small misalignments in the mirror structure and unavoidable loads induced by the vehicle spin. This paper describes an intensive effort to understand and document the performance of the scan mirror bearing system under these loads. This effort involved calculation of the bearing loads and expected friction torque, comparison of the computed values to test data, and verification of the lubrication system performance and limitations under external loads. The study culminated in a successful system launch in February of 1987. The system has operated as predicted since that time.

SYSTEM DESCRIPTION

The GOES 7 spacecraft is a spin-stabilized geosynchronous vehicle which provides near hemispherical images of earth's weather patterns. Storm warnings from this and earlier spacecraft have saved many lives and millions of dollars in property damage. As such, the complete and continuous production of such weather images is a vital national asset. Indeed, almost no evening news telecast is complete without the weatherman's review of the satellite image.

GOES 7 now provides such images using a Visible Infared Spin Scan Radiometer (VISSR). The VISSR can scan the earth once every 20 minutes by using a scan mirror to reflect an image of the earth over a series of photodetectors. The image is built up like a TV image from a series of horizontal lines. Spacecraft spin provides a west to east image motion for the scan mirror. Then while the VISSR is pointed away from earth, the scan mirror is stepped one line from north to south. Thus a series of lines is collected building a complete image of the earth. It is the scan mirror's support bearings which are the subject of this report.

---

* This work was supported by NASA Contract NAS5-20769

** Hughes Aircraft Company, Space and Communications Group
Los Angeles, California

Figure 1 illustrates the scan mirror system. The mirror is attached at four points to a beryllium support structure. This structure is mounted between a pair of motor, ball bearing and optical encoder assemblies referred to here more compactly as encoders. The beryllium support is hard mounted directly to the beryllium shaft of each encoder. The primary encoder is hard mounted to the instrument frame while the redundant encoder is mounted to the frame through a flexible diaphragm as shown. This diaphragm permits axial motion while maintaining high radial stiffness.

Each encoder contains a preloaded pair of angular contact bearings which support the shaft. In operation, the shaft position is sensed by the encoder and compared to a command value. Any error signal is inverted, amplified and supplied to the drive motor. Any mechanical resistance to achieve the desired position is thus sensed as a voltage which is relayed to earth in the telemetry train. Such resistances include inertial and dynamic imbalance effects as well as the various components of ball bearing friction (References 1-4).

The angular contact bearings' solid lubrication system had evolved towards thinner coatings over 10 years. For GOES 7, the coating of molybdenum disulfide was applied by radio frequency sputtering and was only 3×10^{-8} meters thick. This thickness was selected[5] to provide the maximum operational life before the lubricant would form "torque bumps", common in solid lubricated oscillatory bearings. These bumps were believed to form due to the minute, but repeated accumulation of solid lubricant at the ends of the ball path. As will be shown later in this paper, we found that these torque bumps are not simply due to debris accumulation, but may also represent significant race damage.

DESCRIPTION OF VEHICLE TEST ANOMALY

During spacecraft spin testing, the main scan mirror friction torque had to remain below a prescribed maximum throughout the entire mirror scan. During anechoic testing, the mirror drive torque for the spinning vehicle reached a peak of 0.1 N-m. The launch requirement was 0.076 N-m.

A brief test program was conducted on the vehicle to determine the cause of the high friction torque. During the test, it was noted that the mirror drive torque climbed significantly as the vehicle spin speed increased. Test results at 0 and 100 RPM are shown in Figure 2.

INTRODUCTION TO ANALYSIS

The relationship between average scan mirror drive friction and spin speed was examined with the results shown in Figure 3. It was noted that the friction increase with spin rate followed a curve typical of ball bearing friction trend with increasing load.

The encoder bearings are thin section angular contact ball bearings duplexed back to back with beryllium spacers. The bearing geometry and loading are summarized in Table 1. Using the techniques described in Appendix A, we plotted the expected friction torque increase vs. cross-axis moment per bearing pair for these bearings, obtaining the curve shown in Figure 4. The figure also gives mean contact stress levels for the bearings at the indicated loads. Comparing this curve to Figure 3, it can be seen that the loads required to produce the observed mid-frame torque on a single bearing pair are not unreasonably high, and that the operating stress level for the bearings at this load is well below ball or race damage limits for lubricated bearings.

Checks of the motor drive and data acquisition systems indicated that these systems were functioning properly. Other aspects of the testing supported the theory that unexpected bearing loads were the problem.

It did not matter which of several test encoders was installed on the redundant side of the vehicle. The mounting diaphragm on this side (see Figure 1) does not transmit axial or moment loads to the redundant encoder bearings. Also, those cases in which a development model encoder was mounted on the primary side produced consistently low torques. The bearings in this encoder were not preloaded, hence were insensitive to small misalignments. Finally, it was discovered that the bearings on earlier vehicles, which had exhibited a smaller torque increase upon spinup, had been designed with slightly different race curvatures which would reduce the alignment sensitivity. This is discussed in Appendix B.

TEST DESCRIPTION

Having found the probable cause for the observed friction torque, it was determined that it was not possible to quickly change the VISSR/vehicle in such a way to eliminate these loads. The amount of misalignment which would cause the observed friction was well within the likely manufacturing tolerances (see Appendix B). Contact stresses which exist at this load are compared to those which correspond to the design preload in Table 2. The projected mean contact stress levels were not so high that lube failure was by any means certain. However, there was no relevant life data available at these stress levels.

It was agreed with NASA that a two-phase life test should be carried out in parallel with launch preparations. Spare flight quality bearing pairs would be tested at loads which encompassed the worst case loads, calculated from encoder motor drive voltage measurements under load (Appendix C). We needed to develop an understanding of the method and rate at which the lubricant coating would be consumed, and the margin which could be confidently maintained with an available motor

torque of 0.56 N-m. Earlier vehicles in this series had exhibited a small but steady increase in drive friction at each end of the scan. We needed to be certain that this effect would not suddenly become much worse at these higher loads.

The initial test phase was an accelerated life test of twice the mission duration, to verify that there would not be a sudden breakdown of the lubrication system and reduction in life. These bearings were analyzed to determine the performance of the lubrication system at relatively high loads.

The second test phase more closely approximated orbital scan rates, and used a spare encoder for a drive. This phase allowed us to observed the gradual buildup of torque bumps in the system, as well as test possible sequences of scan alteration to preserve the lubricant should this be required on orbit.

The assembly used for life testing the encoder bearing pairs is shown in Figure 5. Several bearing pairs were tested simultaneously. Table 3 gives the test parameters for each phase of testing.

TEST RESULTS

TORQUE HISTORY, PHASE I

The accelerated life test was halted periodically and the mid-frame and end-of-frame torques measured by hand. The results are shown in Figures 6 and 7.

It is apparent that the friction torque response of this lubrication system is highly load dependent. The end-of-frame torque in particular increases dramatically for the loaded bearings between 1 and 1.5 lifetimes. Of even more interest is the difference in mid-frame torque between the two identically loaded bearings. This would indicate that at the stress level shown in Table 2, we are very close to a damage threshold for the lube system. Subsequent analysis of the bearings showed this to be true.

At the end of two lifetimes, the frame limits for the worst of the loaded bearing pairs were extended and the test continued by hand. Figure 8 shows the rate at which the end-of-frame torque decreased during this process. It can be seen that the end-of-frame torque was brought within manageable (0.28 N-m) limits rather quickly, although it did not reach the beginning of life level.

TORQUE HISTORY, PHASE II

The second phase of the life testing used new bearings in the same fixture (Figure 5), except we used a spare encoder to drive the test bearings. Using the VISSR drive electronics, the maximum scan rate was considerably slower than that used in the first test phase. This method resulted in precise repeatability of the frame limits, and in the same step and settle wear dynamics which would occur in flight (see Table 3). This phase offered an opportunity to study the changes in torque over the scan. Changes such as the growth of torque bumps at the end of scan were thought to form due to the repeated deposition or extrusion of solid lubricant at the end of the ball path. Such deposits would decrease the bearings' radial clearance and lead to complex torque/position profiles.

It was initially agreed that torque bump rolldown procedures would be implemented when the total end-of-frame torque (three bearing pairs) reached 0.175 N-m. This rolldown limit was subsequently raised to 0.21 N-m. With this provision, the torque bumps at each frame limit were maintained by shifting the frame limits approximately 0.5° in each direction when required. Figures 9 and 10 show sample torque traces before and after a rolldown. The torque shown is the sum for all three test bearing pairs. It can be seen (Figure 9) that through most of the scan, the average torque remains fairly constant with some lumps and noise. Approaching the CW end of the scan, the required torque drops to zero and then climbs to a peak of approximately .25 N-m. With rolldown, this peak is considerably reduced (Figure 10).

The end-of-frame (CW) torque history of the experiment is shown in Figure 11. The figure indicates that the end-of-frame torque was easily maintained within reasonable limits through simple rolldown procedures. At the end of the test (1100 orbital days), the contribution of each individual bearing pair was measured. The results for the loaded bearings are shown in Figure 12.

POST-TESTING BEARING EXAMINATION

Following the completion of each test, the bearings were disassembled for study. Bearing components were examined by visual and Scanning Electron Microscopy (SEM) as well as limited chemical analysis using Energy Dispensive Analysis of X-Rays (EDAX). Following microscopy, the bearings were mechanically inspected using profilometry.

Examination of the normally loaded bearings from both test phases found the ball path lubricant severely reduced. SEM images showed no signs of distress beyond the partial loss of lubricant. No piles of debris or lubricant were found. A typical view is seen in Figure 13

left. Profilometry did find evidence of race wear, particularly at the ends of travel where the races had worn by as much as 4.1×10^{-7} meters.

The moment loaded bearings did not fare so well. Phase I bearings visually showed wear paths with severity corresponding to ball load. The most heavily loaded balls had very patchy lubricant coatings on the race and some evidence of metallic damage. Serial Number 101 was the worst with large areas of metallic damage as seen in Figure 13 right. Figure 14 shows details of Phase I ball paths. Some ball paths ended in accumulations of lubricant as seen in Figure 14 right, but many more were devoid of lubricant and were just torn up steel as shown in Figure 14 left.

Phase II moment loaded bearings were visually indistinguishable from the normal load bearings; this is consistent with their lower accumulated life and good torque performance to that point.

Circumferential profilometry of the Phase II bearings did not reveal the presence of debris bumps at the ends of scan. Instead, we found wear pits at each end of travel, but only on the outer race as shown in Figure 15. Data from any Phase I loaded bearing showed a badly roughened surface consistent with the surface seen in Figure 13 right.

ENERGY APPROXIMATION

It is informative to calculate the work which should be required to elastically deform a ball rolling through the wear scar of Figure 15 as the bearing is rotated. The normal ball load will tend to decrease as the ball rolls into a wear depression. Conversely, the ball will need to be compressed to fit between unworn sections of the races. This compression/relaxation of the ball will require work which is supplied by torque acting through some angle. The same effect should also occur as the ball rolls over debris in the ball path (see Figures 9 and 10).

A detailed analysis of this action would need to include the race out-of-roundness and the ball size variations, and is beyond the scope of this paper. However, we can compare the magnitude of the torque "bumps" shown in Figures 9 and 10 with the expected torque based on the profilometry data shown above. Under preload alone, the normal approach of the ball to the outer race is approximately one micron. The work stored and recovered in the contact as it is cycled by the 0.6 microns indicated in Figure 15 may be calculated to be approximately seven micro-Joules. Using our torque traces through a scan, we can estimate the work in any of the bumps using the formula as follows:

$$\text{Work (J)} = [\text{Torque (N-m)}/\text{pitch radius (m)}] \times \text{arc-length (m)}$$

This gives in Figure 9 for the CW "bump" growth of 0.15 N-m over 0.002 radians, a work of approximately 300 micro-Joules. This corresponds to some 43 balls climbing out of a depression such as that in Figure 15.

In the Phase II testing, one bearing pair was under moment loading. Under this condition, approximately half of the balls (or 36 of 72) share the load.

CONCLUSIONS

The GOES 7 spacecraft in now on orbit and functioning as designed. Early ground tests indicated that unexpected, higher VISSR bearing loads were present. These loads increased the torque required to drive the scan mirror. Concerns that the high torque might continue to increase led to a search for the cause and testing to demonstrate acceptable performance despite the high loads. Analysis showed that increased torques were due to spacecraft spin and instrument alignment difficulties.

Life of the MoS_2 sputter lubricated film was greater than two mechanism lifetimes under normal loads. Addition of the moment load reduced that life to between one and two lifetimes. Increases in end-of-frame torque due to debris and race wear were found to be manageable by periodic changes to the VISSR frame limits.

It is apparent that there are two major contributors to the observed friction torque behavior of the scan mirror drive. Looking at any of the torque traces (see Figures 9, 10, and 12), we see that there is an average drive torque hysteresis loop on which is superimposed a large amount of low-frequency noise.

The average torque hysteresis represents a frictional loss due to sliding at the ball-race contacts. We have shown that both the magnitude and the load dependence of this term can be readily determined using the methods (and in the case of the software) of Jones (reference 3). The magnitude of this torque is proportional to the coefficient of sliding friction at the interface. This is very apparent from the large increase of average mid-frame drive torque as we wear through the MoS_2 (see Figure 6). For new bearings with this lubrication system, a coefficient of sliding friction of 0.16 is appropriate. This implies that some metal-to-metal contact is occurring even at the beginning of life.

The second contributor to the system drive torque is the work which much be done to roll over the debris and through the wear scars which develop as the lubricant film wears. This friction is not a loss term; the elastic nature of the ball compression is evident in the manner in which the CW and CCW torque traces of Figures 9 and 10 parallel one another.

ACKNOWLEDGEMENTS

The authors wish to thank Hughes Aircraft Company and the National Aeronautics and Space Administration for permission to publish this study. We also thank F. Malinowski and L. Kubel of Santa Barbara Research Center for many discussions and for performing or assisting in many of the tests needed to complete this work. Finally, we thank K. Silva for her patience in helping us with the manuscript preparation.

REFERENCES

1) Mullin, J.V., and Speece, A.L., "Prediction of Bearing Torque Variation Based on Profilometry Data", ASME 69-WA/Lub-4, November 1969.

2) Dahl, P.R., "A Solid Friction Model", SAMSO Report TR-77-131, DTIC Number AØ4192Ø, May 1968.

3) Jones, A.B., "The Mathematical Theory of Rolling-Element Bearings" in "Mechanical Design and Systems Handbook", H.A. Rothbart, ed., McGraw-Hill, 1964.

4) Stevens, K.T., and Todd, M.J., "Experiments on the Torque of Ball Bearings Over Small Angles of Moment", ESA/ESTL/34, Risley, England, 1979.

5) Christy, R.I., and Barrett, G.C., "Sputtered MoS_2 Lubrication System for Spacecraft Gimbal Bearings", Lubrication Engineering, Volume 38, 8 437-443, 1978.

APPENDIX A - BALL BEARING FRICTION

THEORETICAL SUMMARY

The computation of ball/race sliding friction under load involves a numerical integration of the frictional forces generated across each contact zone. In preparation for this, the individual ball loads, pressure ellipse dimensions, orientations, and motions must be determined. This is a formidable computational effort and we have used the A.B. Jones ball bearing analysis program for the task. Reference 3 gives details of the analysis which is summarized here.

In any ball bearing, the pressure ellipse has a marked curvature in the plane of the major axis. This curvature is the major cause of sliding friction in ball bearings. Integrating the frictional forces across the contact zone, we may determine a net moment about an axis which skewers the curved pressure ellipse for each ball/race contact.

The sum of these torques for all of the contacts in the bearing provides the major source of bearing rolling friction.

In a radial bearing under radial load, the contact zones at each race may be described as above. In the case of an angular contact bearing, at least one race will have a spinning motion superimposed upon the rolling motion, giving rise to additional frictional forces. These forces can also be integrated over each contact area to determine a net contribution to bearing friction torque. Typically, the spinning motion described will occur at only one race. The race which rolls without spin is termed the 'controlling' race. We found rather dramatic differences in the wear which occurred in the presence of ball spin compared to that on the controlling race (see Figure 15).

APPENDIX B - BEARING RACE CURVATURE EFFECTS

The encoder bearings are mounted back-to-back to provide maximum stiffness for an individual encoder. Unfortunately, with two encoders defining the mirror axis, each must accommodate some slight angular misalignment of its preferred axis.

The bearing manufacturer which had been used for early GOES vehicles stopped producing these bearings and with this change the program received bearings with slightly tighter race curvatures (greater ball/race conformity). Using the methods of Jones, the effect of a few percent change in race curvature can have a significant effect on the sensitivity of the bearing friction to misalignment. This is shown in Figure B-1.

The GOES 7 encoders are mounted on a flange of approximately 0.06m in diameter. A misalignment of 100 microradians corresponds to a flange runout of only six microns. The VISSR is a very complex and stiff structure. It is quite likely that the primary encoder bearings had to accommodate the loads discussed above.

APPENDIX C - EXPERIMENTAL VERIFICATION

In support of the GOES 7 vehicle, the flight encoders were retro-fitted with new bearings having maximum race curvatures. During final encoder buildup, the units were calibrated to determine the individual motor characteristics and bearing pair sensitivity to external loads. Based on this information, we were able to more accurately calculate the loads existing in the final spacecraft assembly and verify that they were less than those of the life test.

These results correlate well with the ball bearing friction torque calculated for new bearings using the methods described above. The results are summarized in Figure C-1 for moment loads.

TABLE 1 BEARING GEOMETRY AND LOADING

BEARING TYPE	THIN SECTION ANGULAR CONTACT
MATERIAL (BALLS)	AISI 440C STAINLESS
MATERIAL (RACES)	AISI 440C STAINLESS
SPACING	.0518m
PRELOAD	222N (DB)
NUMBER OF BALLS	36
BALL DIAMETER	.00476m
PITCH DIAMETER	.0735m
O.R. CURVATURE	53%
I.R. CURVATURE	52%
CONTACT ANGLE	0.3 radians

TABLE 2 BALL-RACE MEAN CONTACT STRESS (MPa) (HEAVIEST LOADED BALL)

	OUTER RACE CONTACT	INNER RACE CONTACT	ELLIPSE CONTAINMENT
PRELOAD	587	570	100%
TEST LOAD (63 N-m)	997	969	100%

TABLE 3 LIFE TEST PARAMETERS

	PHASE I	PHASE II
EXCURSION	.175 radians (10°)	.175 radians (10°)
DURATION	245,000 Cycles	58,000 Cycles
VELOCITY	Sinusoidal, 0.2 Hz	Mid-frame (± 860 lines): Retrace Frame end (last 50 lines): Normal
TEMPERATURE	21°C	21°C
PRESSURE	1×10^{-6} Torr	1×10^{-6} Torr

NOTE:

Retrace velocity is .00017 rad/sec average.
Normal scanner velocity is 0.000016 rad/sec average.

Both normal and retrace are stepping motions. Step duration is approximately 0.05 seconds.

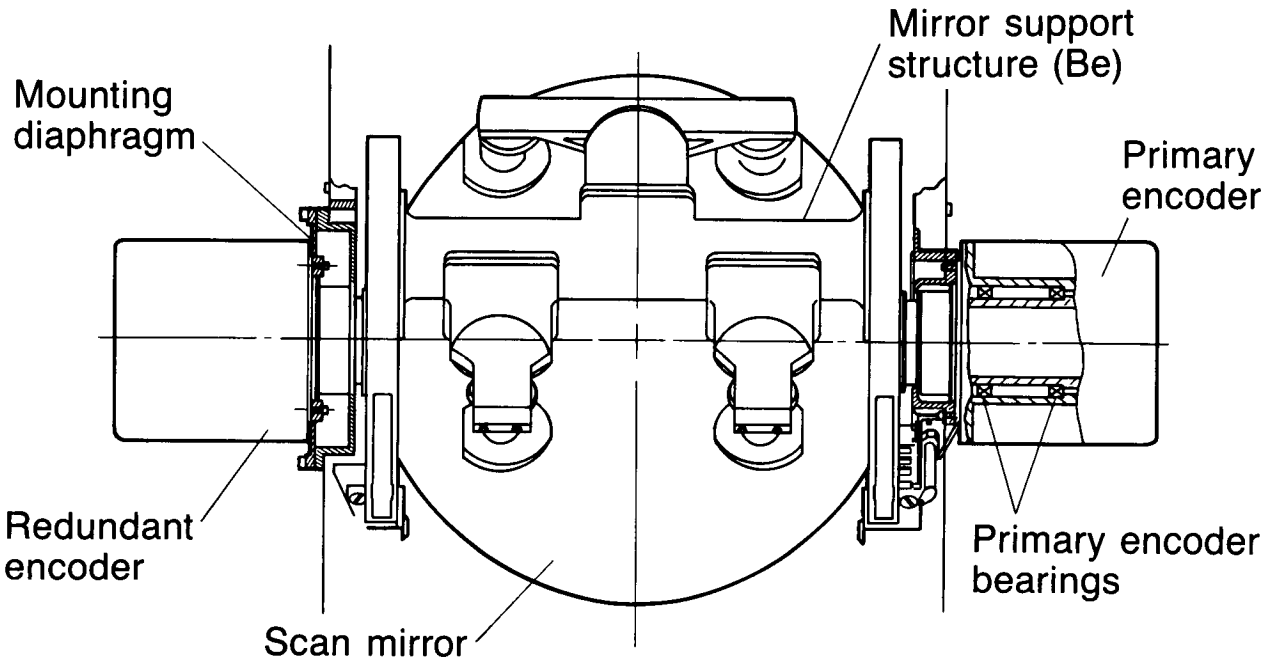

FIGURE 1. GOES-7 SCAN MIRROR DRIVE

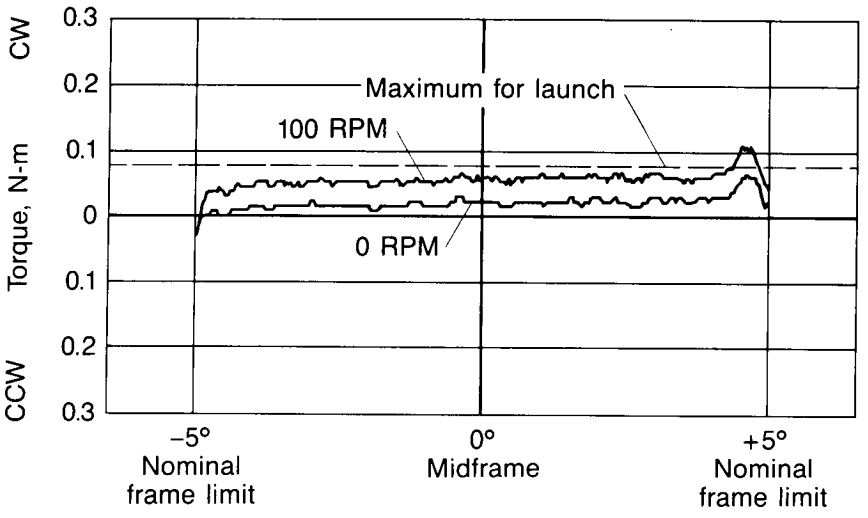

FIGURE 2. TORQUE THROUGH SCAN — ANECHOIC TESTING

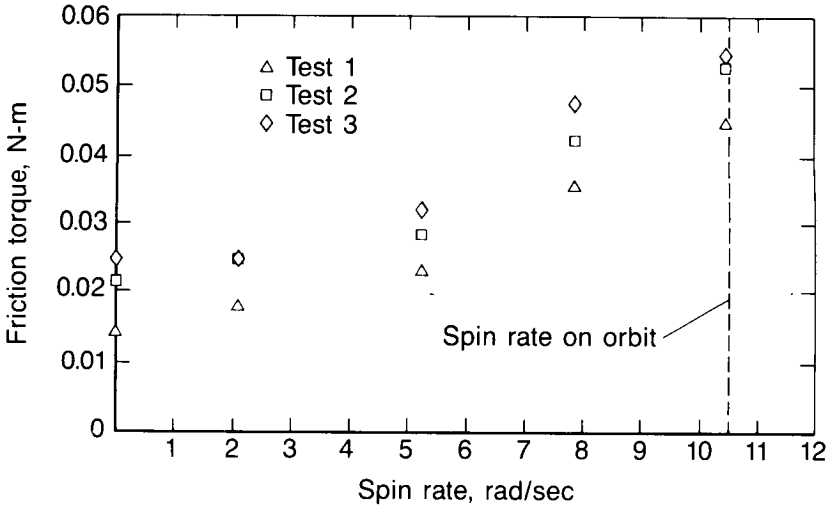

FIGURE 3. FRICTION TORQUE vs VEHICLE SPIN RATE

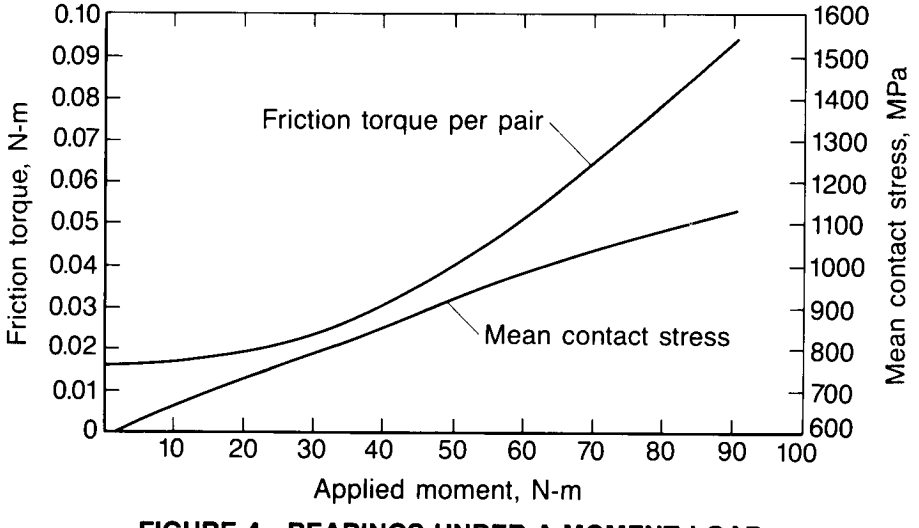

FIGURE 4. BEARINGS UNDER A MOMENT LOAD

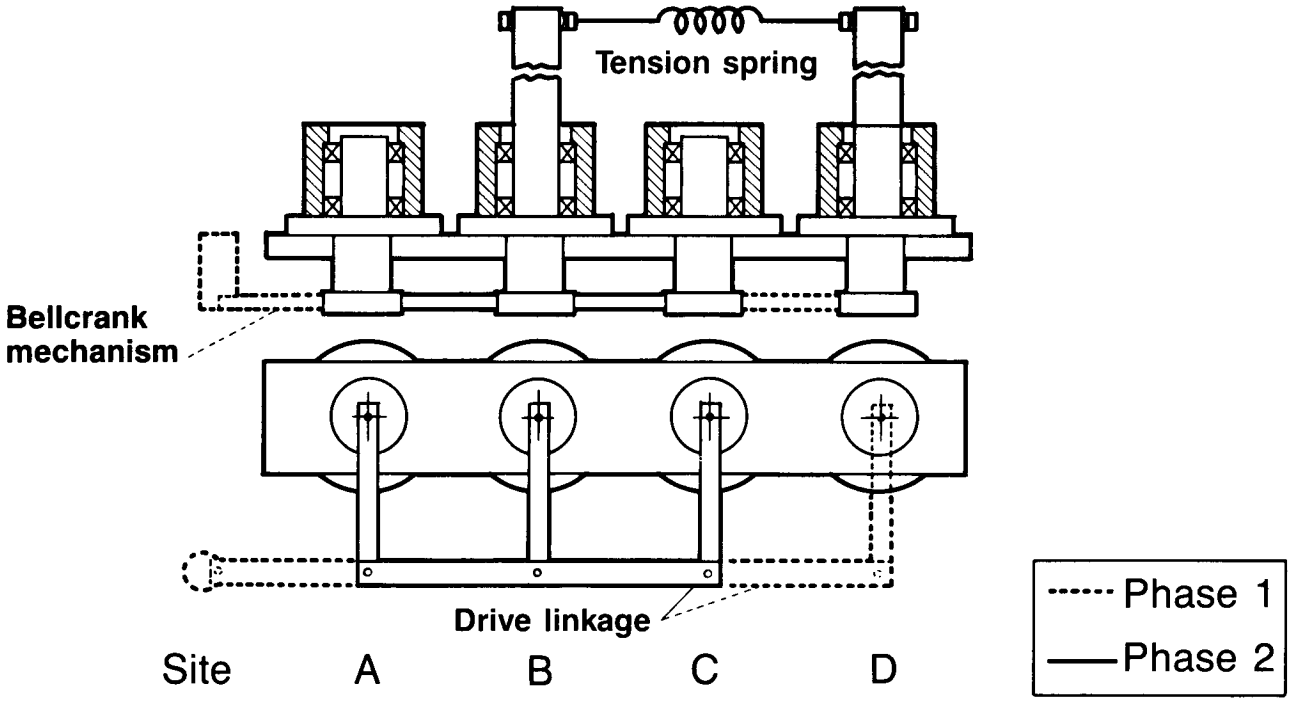

FIGURE 5. EXPERIMENT SCHEMATIC

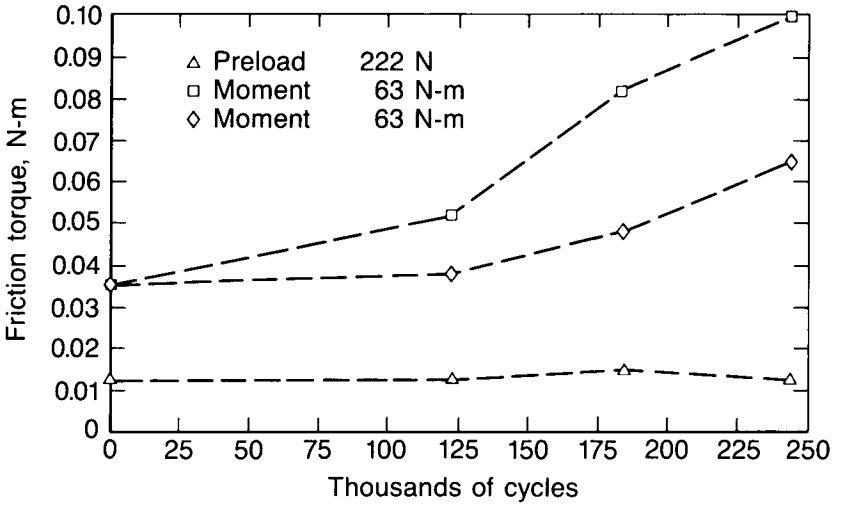

FIGURE 6. ACCELERATED LIFE TEST RESULTS — MIDFRAME

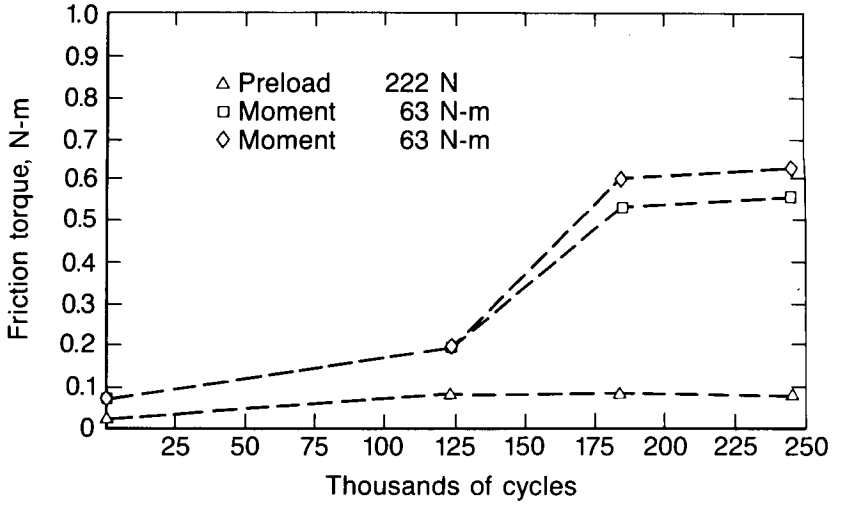

FIGURE 7. ACCELERATED LIFE TEST RESULTS — END-OF-FRAME

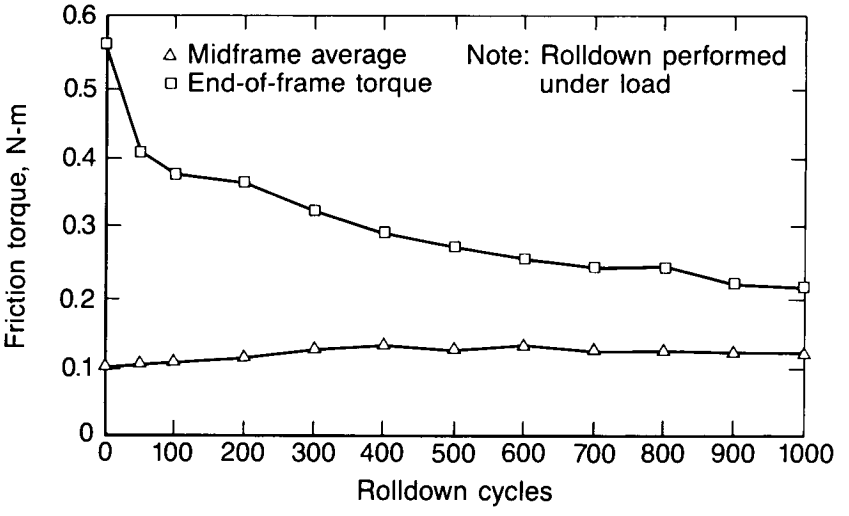

FIGURE 8. POST-ACCELERATED LIFE TEST MANUAL ROLLDOWN

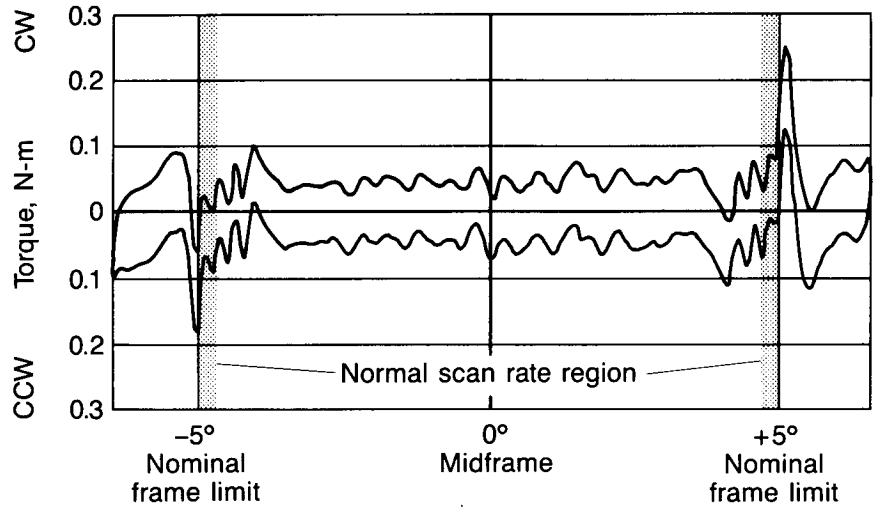

FIGURE 9. LIFE TEST PHASE II (943 DAYS) — TORQUE TRACE BEFORE ROLLDOWN

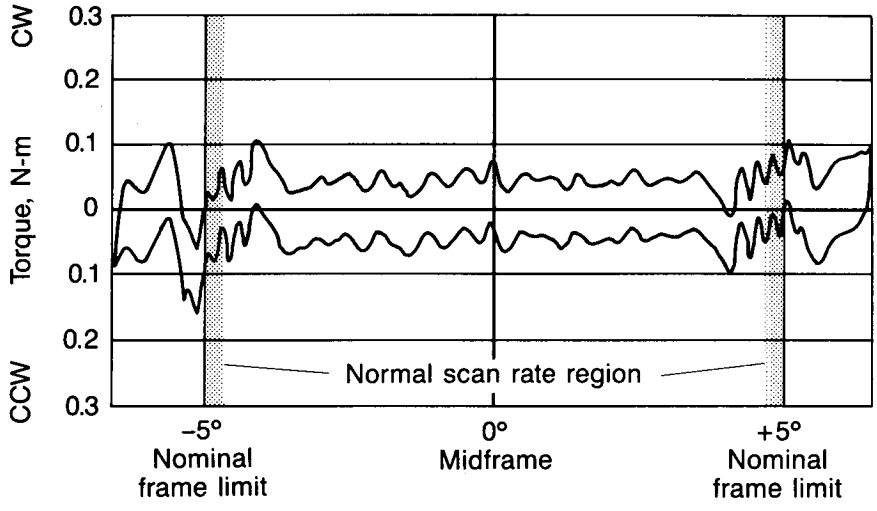

FIGURE 10. LIFE TEST PHASE II (943 DAYS) — TORQUE TRACE FOLLOWING ROLLDOWN

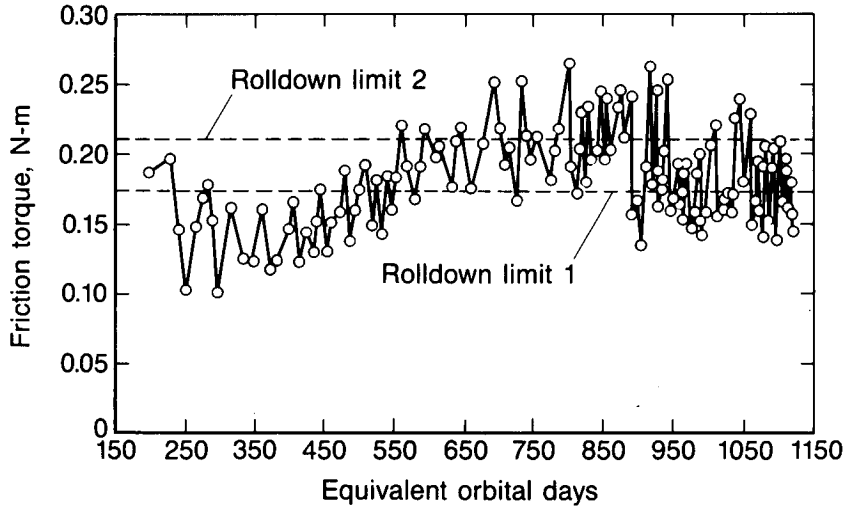

FIGURE 11. LIFE TEST: PHASE II TORQUE HISTORY — CLOCKWISE END-OF-FRAME PEAK TORQUE

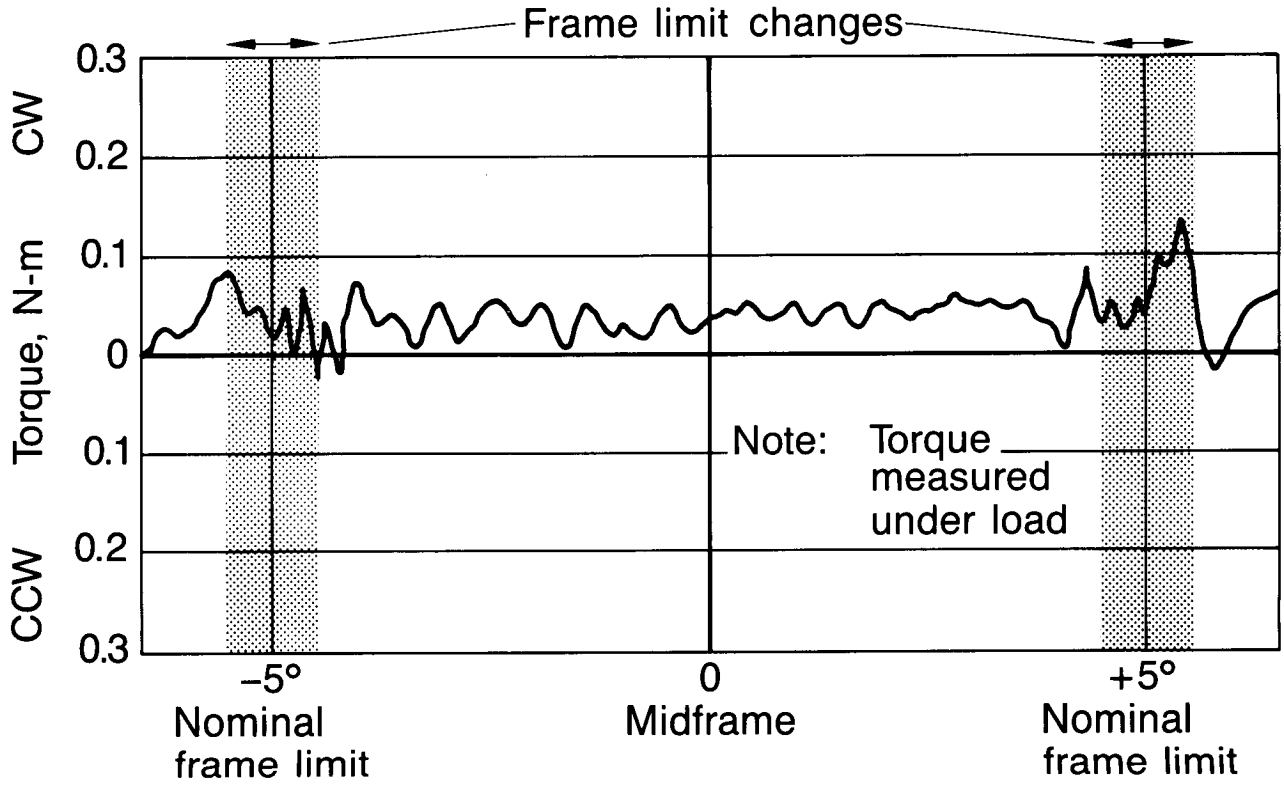

FIGURE 12. TORQUE FOLLOWING PHASE II TESTING — MOMENT LOADED PAIR

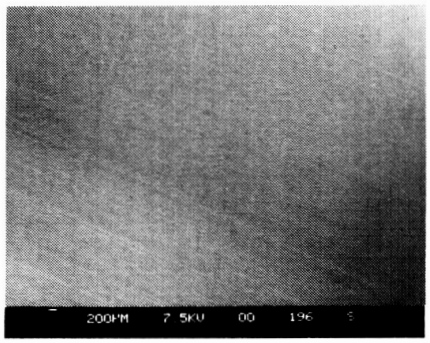

Phase II bearing showing "hole" and typical surface condition

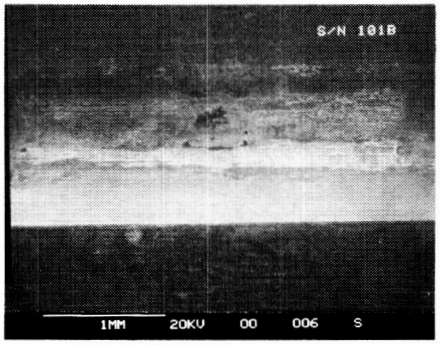

Phase I bearing showing damage in ball path

FIGURE 13. OUTER RACE BALL PATHS (SEM)

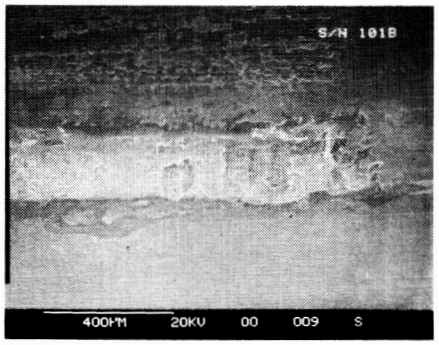

Showing metal damage but no lubricant buildup

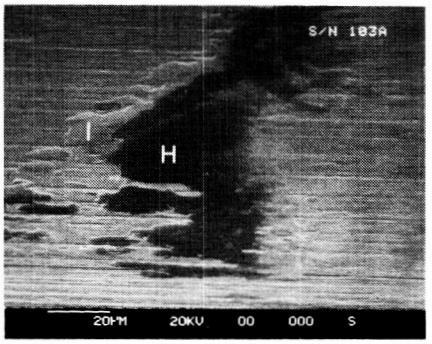

Showing lubricant buildup Region I is earlier accumulation with less steel wear debris than H

FIGURE 14. END-OF-FRAME BALL PATH DETAILS

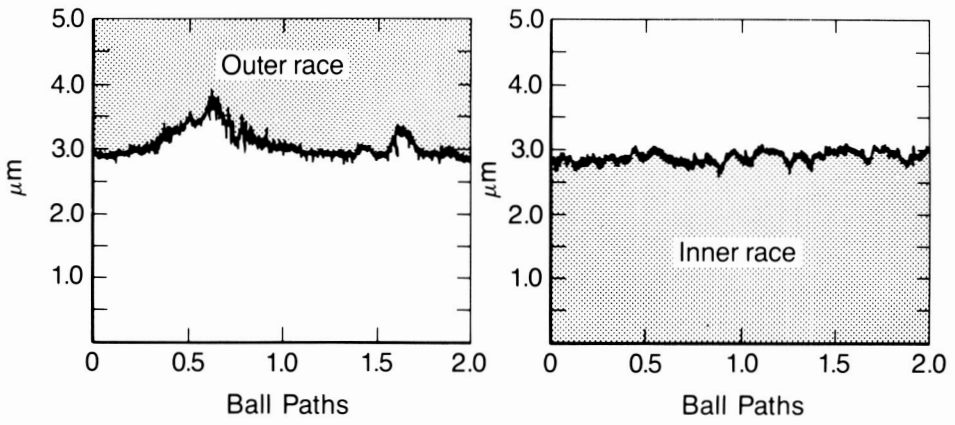

FIGURE 15. TYPICAL WEAR SCARS FROM MOMENT-LOADED BEARING

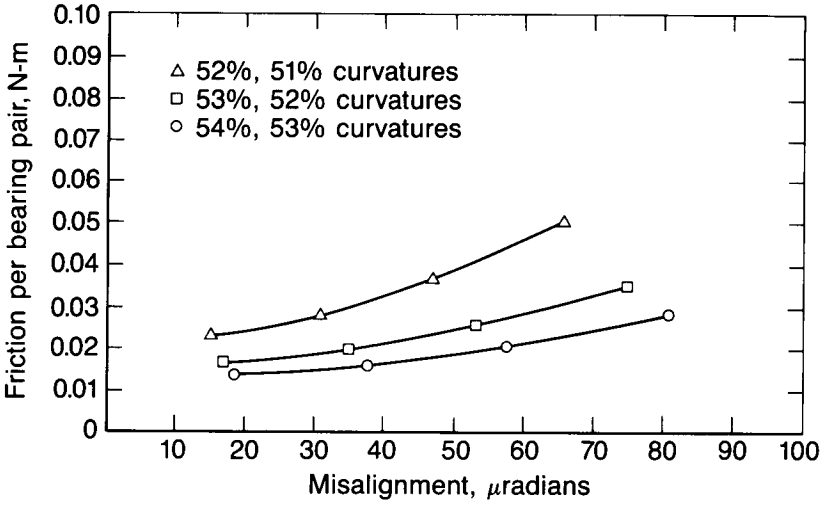

FIGURE B1. RACE CURVATURE EFFECTS

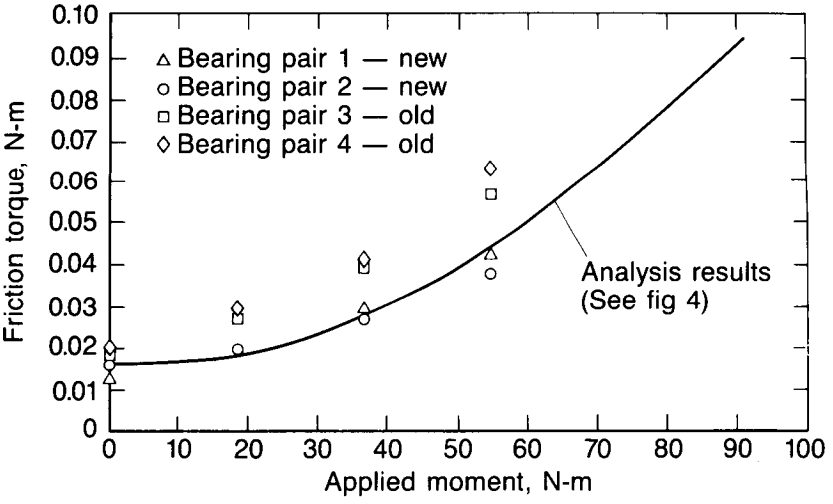

FIGURE C1. BEARINGS UNDER A MOMENT LOAD — TEST